플라스틱 파이프의 잔류응력에 관한 연구
III. 정적균열성장 거동에 미치는 영향

최　선　웅†·Lawrence J. Broutman*

한남대학교 고분자학과, *미국 브라우트만사

(1996년 11월 4일 접수)

Residual Stresses in Plastic Pipes and Fittings
III. Effect on Stable Crack Growth Behavior

Sunwoong Choi† and Lawrence J. Broutman*

Dept. of Macromolecular Science, Hannam University, Taejon 306-791, Korea
*Broutman and Associates Ltd., Chicago, Illinois 60616, USA

(Received November 4, 1996)

요 약: 플라스틱 파이프 구조물에 존재하는 잔류응력과 분포가 파이프의 성능과 밀접한 관계를 이루는 정적균열성장 거동에 미치는 영향에 대해 살펴보았다. 본 연구에서 개발된 시험방법은 파이프 내의 잔류응력을 원상태 그대로 균열성장에 적용하는 방법으로서, 폴리에틸렌 파이프로부터 얻어진 링모양의 시편에 plane-strain상태의 균열이 개시될 수 있는 최소 길이의 크랙 (0.5 mm)을 시편내의 압축 또는 인장 잔류응력에 노출시켜 균열 성장속도를 측정하였다. 인장 잔류응력 상태로부터의 성장속도는 압축 잔류응력에서 보다 약 3배 빠른 속도로 진행되는 것이 관찰되었고, 이에 대한 물리적 증거는 파괴 표면에서 크랙 전면모양으로부터 얻을 수 있었다. 처음 균열 길이에서의 응력확대인자는 압축잔류응력에 노출되었을 경우 300 $KPa\sqrt{m}$ 이었으며, 아닐링에 의한 무잔류응력상태에서는 550 $KPa\sqrt{m}$로 측정되었다. 이로서 잔류응력은 정적균열성장의 추진력인 응력확대 인자에 큰 영향을 주는 것을 알 수 있었다.

ABSTRACT: The effect of residual stresses on stable crack growth (SCG) behavior in polyethylene pipes was investigated. For the investigation, a new SCG specimen and test method were developed which offered a promise for characterizing the slow crack growth behavior in pipe sections without disturbing the existing residual stress state. The specimen was in the form of diametrically loaded ring, obtained from a pipe, having a notch either at outer surface or at inner surface, corresponding to a state of compressive and tensile residual stresses, respectively. It was demonstrated that crack growth from the compressive stress region was delayed due to circumferential compressive residual stress while accelerated under the tensile residual stress. In the absence of residual stress the slow crack growth was independent of whether the crack was initiated at inner or outer surfaces. The estimated stress intensity factors for the outer notched samples were 300 $KPa\sqrt{m}$ and 550 $KPa\sqrt{m}$ for as received and annealed pipes, respectively, clearly demonstrating the value of SCG specimen with regard to residual stress effect on the crack driving force. The physical evidence for the residual stress effect is presented from the respective crack front shapes.

Keywords: plastic pipe, ring SCG specimen, residual stress and distribution, slow crack growth.

Sunwoong Choi and Lawrence J. Broutman

INTRODUCTION

The effect of residual stresses on the behavior of materials has been reasonably well studied in the case of traditional materials like metals and ceramics. However, unfortunately, such study has not been so extensive in polymers and in particular a very limited study exists on slow crack growth behavior.[1,2] One reason why the residual stresses in polymers have been neglected may be related to their magnitude. The maximum values of residual stresses that can exist are always limited by the yield stress of the materials since stresses in excess of the yield strength are relieved by the plastic flow. The yield strength of an organic polymer is generally much less than that of a metal or a ceramic glass. Thus, the residual stresses in a polymer may appear insignificant compared to those found in metals and ceramics. It is now recognized that their relative effect on materials behavior is the same independent of the material system. Depending on the sign, magnitude and the distribution of the residual stresses with respect to the superimposed external stresses, it can be either beneficial or detrimental. Beneficial if one can control in a way by which they can be selectively introduced in the areas needed. However, in most cases, if possible, one would like to avoid internal stresses for the simple reason that for many documented cases, the residual stresses were the predominant factors contributing to these failures.

In plastic pipes and fittings for low and medium pressure applications, the most important material characteristics governing the field failures are the crack initiation and the subsequent rate of slow crack propagation.[3-13] The resistance to these two characteristics basically determines the lifetime performance of the plastic pipe and fitting structures. The slow crack can occur in stress intensity factors well below the critical stress intensity fac-

tor, hence any influences that change the stress intensity factor, such as the residual stress, can have profound effect on the slow crack growth behavior. The authors have shown that the residual stresses are present in these pipes and fittings and reported that a maximum biaxial tensile residual stresses were present at the inner surface and a maximum biaxial compressive stresses at the outer surface of the pipes.[14] It was also shown that the initiation and the slow crack growth are very much dependent on the condition and the stress state that exist at the surface.[2,15] Hence, it is expected that the crack initiation and the rate of slow crack growth behavior from each of the surfaces will be different from each other.

To systematically solicit the residual stress effect on deformation and fracture behavior one needs to either find a technique to either methodically vary the residual stress state, or to use a methodology of testing the effect without changing the original stress state and its distribution. The former requirement is more difficult to achieve because the fact that techniques such as annealing create changes not only the residual stress state but also the material property, like crystallinity of the polymer, which also has influence on the mechanical behavior. With regard to this, authors reported that the crystallinity changes from annealing affected primarily the deformation related properties, while the residual stress change was the dominant factor influencing the fracture behavior.[16] In this paper, results relating the residual stress to crack initiation and slow crack growth in residually stressed polyethylene pipes used for the natural gas distribution system are presented. A new slow crack growth (SCG) test specimen will be described, which offers promise for characterizing crack initiation and growth in plastic pipe sections without disturbing the existing residual stress state.

DEVELOPMENT OF SCG RING SPECIMEN

The investigation of the stable crack growth behavior in materials involves the study of crack initiation and propagation, generally under the mode I fracture geometry. Thus to measure the effect of residual stresses on mode I slow crack behavior in a residually stressed pipes, ring samples sectioned from the pipes having notches in residually stressed locations, and loaded in diametrical compression was investigated (Fig. 1). Through thickness circumferential residual stress distribution in PE2306IA 2SDR11[17] ring samples, measured by the turning and boring methods[14] is illustrated in Fig. 2. A compressive hoop residual stresses exist near the outer surface and tensile near the inner surface. Thus, when the notches were introduced at positions 1 and 2 (Fig. 1), the notch tips became exposed to a compressive and a tensile residual stress states, respectively. The magnitude of the residual stress at the notch tips depended on the length of the notch introduced. In an equilibrium system, forces from the residual stresses having different signs need to balance, and the force balance can be expressed as shown in Equation 1.
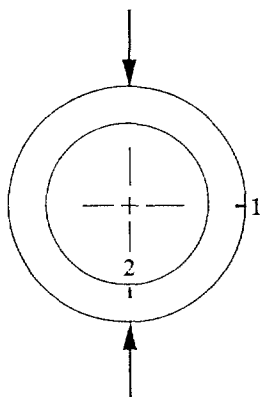
$$\int_0^{h_0} \sigma_\theta(h)\,dh = 0 \tag{1}$$

Here, σ_θ is the circumferential residual stress, and h and h_0 are the current wall thickness and original wall thickness of the ring sample, respectively. Hence, to maintain the equilibrium with an introduction of a notch, the residual stress state need to redistribute. This implies that to minimize the change of the original residual stress state, the notch depth introduced should be as small as possible, however not too small so that the plane-strain crack initiation becomes difficult to achieve. For this, a notch depth of 0.5 mm was experimentally established and this would expect to cause about 4% change at the each ends of the residual stress distribution. Thus, for all practical purposes, by using the ring specimen with a 0.5 mm notch, the residual stress effect can be tested without changing the original stress distribution. Also, to produce plane-strain slow crack growth, a ring sample width of 25 mm was employed.
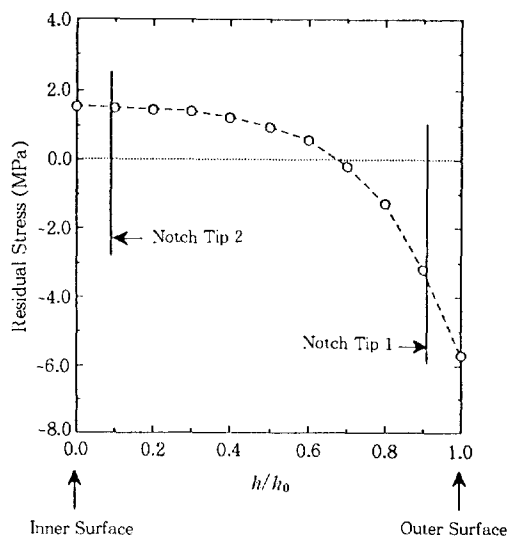
To insure the effectiveness of the SCG ring

Figure 1. Notched ring specimen geometry for SCG testing.

Figure 2. Through wall thickness residual stress distribution in as-received PE2306IA 2SDR11 pipe.

sample, relationship between the applied diametrical load and the stress magnitudes developed at notch positions 1 and 2 were determined. For this an experimental analysis on ring samples prepared from PE2306IA pipe and 2024AL alloy bar stock, both having 2SDR11 dimensions and 25 mm ring width, was preformed. The samples were strain gaged at positions 1 and 2 and tested in a load controlled diametrical compression. The applied force and the corresponding circumferential strains developed at positions 1 and 2 were simultaneously monitored. The results from PE2306IA and aluminum ring samples are presented in Fig. 3, in term of strains at positions 1 and 2. For both specimen types, under a given applied load, the strain at position 2 was twice the strain at position 1, as indicated by the slopes of the respective curves. This implies that the stress produced at position 2 was twice as large in magnitude as compared to position 1. This result was in agreement with the theory based on mechanics[18] and photoelasticity[19] which also predicted the stress ratio between respective positions for rings having the same inner and outer radius. Thus, to

produce a meaningful slow crack growth data, using cracks initiating from surfaces containing residual stresses, it was necessary that a same stress magnitude be produced at both notch positions upon diametrical loading. This was accomplished by subjecting two samples of position 2 notched specimen at a time in a single loading fixture, while one sample per test fixture was used for the position 1 notched samples.

EXPERIMENTAL

Material. The material investigated was the medium density PE2306IA polyethylene pipe grade resin.[17] The pipes were received as-extruded in 2SDR11 size (i.e. 50 mm nominal diameter and the standard dimensional ratio (SDR)-outside diameter to pipe wall thickness ratio of 11). Some of the pipes were annealed at 120 ℃ for 1 hour to eliminate the residual stresses.

Residual Stress Measurements. The circumferential residual stresses both in as-received and annealed pipes were determined by using the combined method of turning and boring techniques, presented in detail in the Part I of this paper series.[14] Same procedures described in Part 1 were also followed for the ring sample preparation. The ring samples from the annealed pipes were sectioned following thermal annealing. The residual stress data obtained was calculated for the through wall thickness distribution using Equation 2. Here, δ is the gap displacement and δ' is the differential δ with respect to the current wall
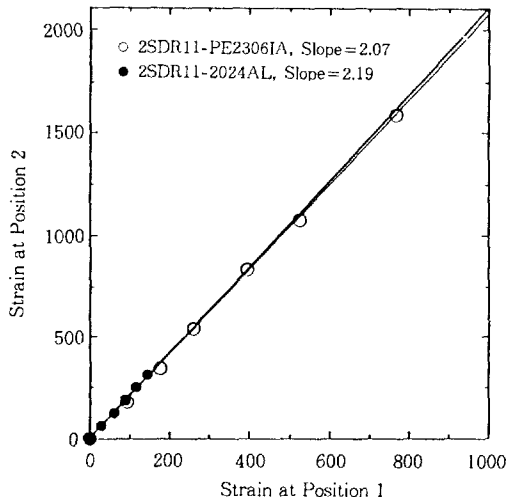

Figure 3. Experimental strain calibration curves for 2SDR11 PE2306IA and aluminum rings.

$$\sigma_\theta(h) = \pm \frac{E(t)}{12\pi \phi^2} \left\{ 4h\delta(h) + h^2\delta'(h) \right. \tag{2}$$

$$+ 2\int_0^h \delta(h)\,dh - \frac{1}{h_0}\left(4\int_0^{h_0} h\delta(h)\,dh \right.$$

$$\left. + \int_0^{h_0} h^2\delta'(h)\,dh + 2\int_0^{h_0}\int_0^h \delta(h)\,dhdh \right)\right\}$$

thickness h. The plus and minus signs preceeding the right hand side represent turning and boring methods, respectively. Also, for turning and boring, ϕ is the inside and outside ring diameters, a and b, respectively. Equation 2 is evaluated by $\delta(h)$ and $\delta'(h)$, which are the quantities experimentally determined.

Slow Crack Growth (SCG) Measurements. The slow crack growth behavior in as-received and annealed pipes was investigated by using ring samples having 25 mm width and notch depth of 0.5 mm. Two types of ring samples were prepared. In one type, the notch was placed at position 1, and in the other type at position 2, corresponding to notch at compressive and tensile residual stress fields, respectively (Fig. 2). The notch was placed across the full width of the ring and perpendicular to circumferential direction, using a razor blade in a specially designed notching fixtures. Notching procedure was standardized as to the penetration rate of the razor blade and the dwell time, and the notch depth produced was monitored with an optical microscope and further checked with the vertical micrometer on the milling table. Also, after the test, the initial notch length was again checked from the fracture surface. The slow crack growth experiments were performed under diametrical compression on ring samples in a 25 v% Igepal-75 v% deionized water solution at a temperature of 50 ± 0.5 °C. A constant diametrical compressive force of 445 N was applied on the ring sample using a pneumatic cylinder, and the load was controlled to ± 0.5 N through a strain gage load cell system attached to the same pressure line. The sample with notch at position 1 was loaded at points 90 °C from the notch, while parallel to notch was employed with position 2 notched specimens. Also, for the latter specimens, two samples were tested simultaneously in a single test fixture, as shown in Fig. 4. The slow crack growth measurements were
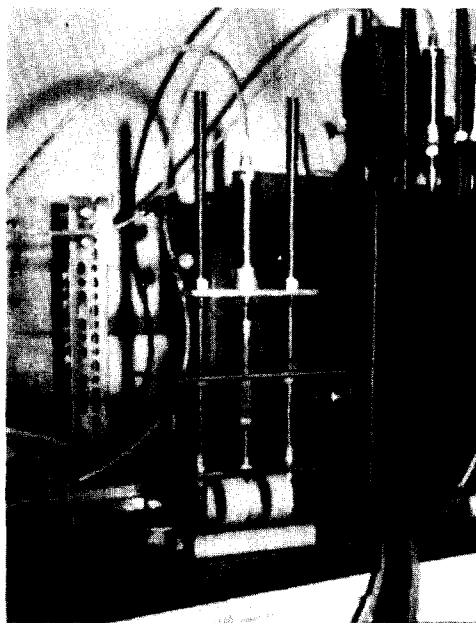

Figure 4. Loading fixture for SCG testing.

achieved by monitoring the crack extension with time. For this, samples were taken out at intervals of the load duration time up to where there was a substantial crack extension through the wall thickness. The ring samples were then washed in distilled water to remove Igepal and impact fractured in liquid nitrogen to reveal the fracture surfaces. The crack length at various load duration times was obtained from the fracture surface by measuring the crack length at several different locations of the crack front, using a traveling microscope (30X), to a resolution 0.01 mm. To represent statistically averaged data, multiple specimens were tested for each load-duration time.

RESULTS AND DISCUSSION

The residual stress state at the tip of the 0.5 mm razor notch in as-received SCG specimen is shown in Fig. 2. Introduction of the notch is expected not to alter the original hoop residual stress distribution throughout the wall thickness,

except near the notch planes created, as was discussed before. Thus, notch tip at position 2 where crack initiation is to begin is surrounded by a tensile residual stress not too different from its maximum value at the inner most surface. Similarly, at the notch tip position 1, a compressive residual stress is present, although because of the stress gradient, some what less magnitudo exists compared to the one at the outer most surface. Thus, for the same applied stress, the total tensile stress available at the notch tip 2 is greater than for notch tip 1 in as-received specimens, while in the case of annealed rings the total stress for driving the cracks at both locations should be approximately the same since the residual stresses have been removed during prior thermal annealing (Fig. 5). As a consequence, the crack initiation and the slow crack growth behavior in as-received and annealed pipes are anticipated to be different, as their fracture behaviors are influenced by the differences in signs and magnitude of the residual stresses present at the repective notch tips.

The slow crack growth results obtained from the as-received and annealed (120 ℃, one hour) ring specimens are illustrated in Fig. 6 for position 1 and 2 notches, in terms of crack length versus the loading time. Distinct differences in the crack growth behavior can be observed between the annealed (zero residual stress) and as-received pipes, and between the crack growth initiating from notches 1 and 2. For example, the crack growth starting from the outer surface (notch position 1) in the annealed specimen is much faster than for the as-received specimen. Also, a substantial incubation time for crack initiation exist in the as-received specimens, while there may be a short incubation time present in the annealed specimens. Such differences in the slow crack behavior between these specimens can be attributed to differences in the residual stress state at the
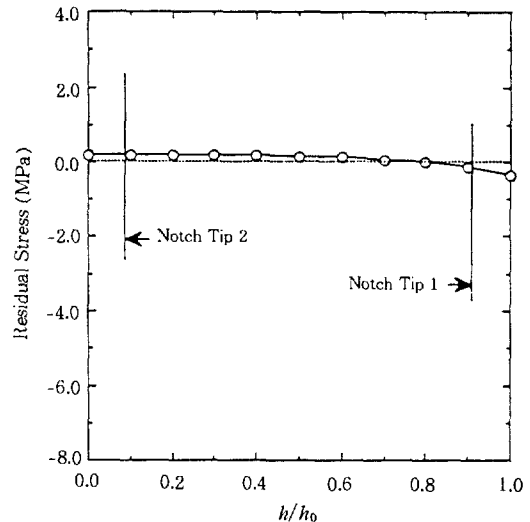

Figure 5. Through wall thickness residual stress distribution for 120 ℃, 1 hour annealed PE2306IA 2SDR11 pipe.
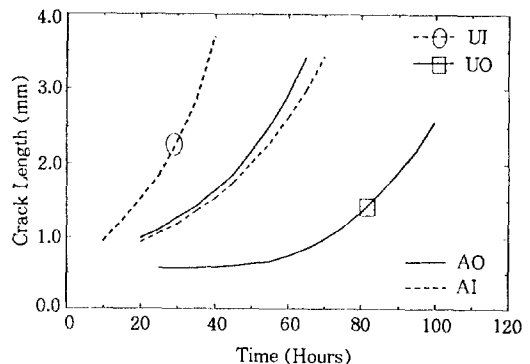

Figure 6. Slow crack growth behavior in as-received and annealed pipes at notch positions 1(outer notch) and 2(inner notch). (UI) as-received/inner notched, (UO) as-received/outer not-ched, (AO) annealed/outer notched, and (AI) annealed/inner notched.

notch tips, where the compressive stress was no longer present in the annealed specimen due to prior annealing. Similarly, the slow crack growth starting from the inner surface notch tip (position 2) is less for the annealed specimen, again consistent with the fact that tensile residual stresses are

removed. It also appears from the shape of the curves, that the incubation time for crack initiation may have been eliminated for the as-received /inner notched specimen, while a short incubation may exist in the annealed specimen. For example, to achieve a slow cracked length of 2.5 mm, it takes about three times less for the notch in the tensile residual stress field (inner notch, as-received) than the notch in the compressive field (outer notch, as-received). Similarly, for the same crack length, about 100% increase in the slow crack growth time can be observed with annealed specimen (zero residual stress), as compared to inner notched, as-received specimen. These results clearly demonstrate the relationship between the residual stress state and the rate of crack initiation and propagation. Hence, in view of the fact that the long-term field performances of the polyethylene pipes are closely related to the rate of crack initiation and slow propagation through the pipe wall thickness, these results provide a direct indication that depending on the existing residual stress conditions in pipes and fittings, their structural performance will similarly vary. Fig. 6 also shows that for annealed specimens the crack growth behavior is independent of whether the crack growth was initiated from the inner or the outer surface. This result verifies that the applied stresses at the notch locations 1 and 2 were indeed approximately the same for the experimental method developed and utilized during this work, as was previously described in the section dealing with the specimen development.

Physical evidence that the slow crack growth is influenced by the residual stress can be seen from the fracture surfaces shown in Fig. 7, 8 and 9 for annealed outer notched, as-received outer and inner notched slow cracked specimens, respectively. The shape of the crack front, during progressive slow crack growth shown for the annealed specimen (Fig. 7) is a typical indication of
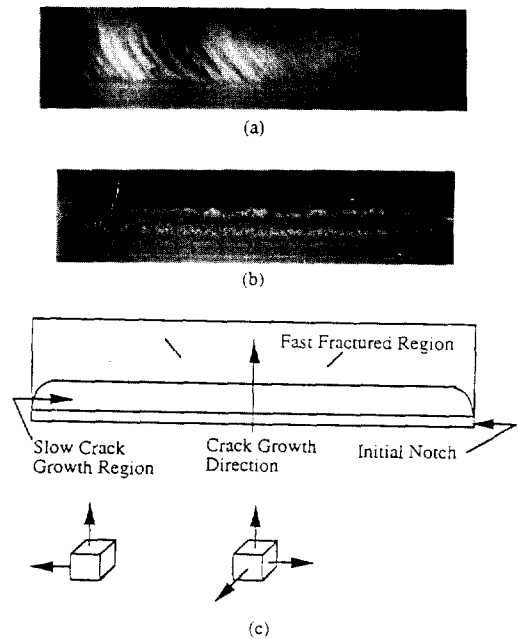

Figure 7. Fracture surfaces of outer notched (notch 1) annealed specimens at various load duration times. (a) $t=t_1$, (b) $t_2>t_1$, and (c) approximate crack tip stress states.

plane-strain fracture being occurred. Similar plane-strain crack front shape was also obtained for the annealed inner notched specimen. This is expected because for the annealed samples the imposed crack tip stresses were tensile and that no residual stresses existed. For as-received outer notched specimens (Fig. 8), the crack grows faster near the edges than at the center region, while the opposite is true for the as received inner notched specimens (Fig. 9). The shape of the crack front clearly indicate the residual stress effect in that while the compressive residual stress at the crack tip acts to retard the slow crack growth, tensile residual stress accelerates the growth. Since the rings were cut from the pipe, the residual stresses in the ring axial direction were relaxed in the region near the ring edges. Hence, the slow crack growth was faster at the
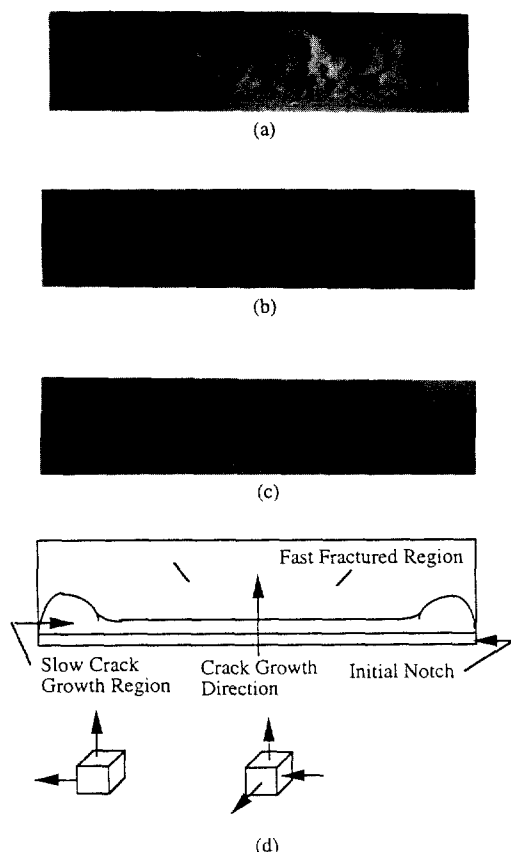
(a)

(b)

(c)

(d)

Figure 8. Fracture surfaces of outer notched (notch 1) as-received specimens at various load duration times. (a) t = t_1, (b) $t_2 > t_1$, (c) $t_3 > t_2$, and (d) approximate crack tip stress states.

sample edge region than the center region due to partial compressive residual stress removal (Fig. 8), while, initially no crack growth was observed at the edge regions due to tensile residual stress removal (Fig. 9). It is interesting to note that for the as-received outer notched specimen, when the crack growth reaches the regions of low compressive residual stress or the beginning of the tensile residual stress state at the notch tip (Fig. 2 and 8), the crack at the center portion begins to grow faster than the edge region, as such that it takes on the shape typical of the plane-strain fracture (Fig. 8c).
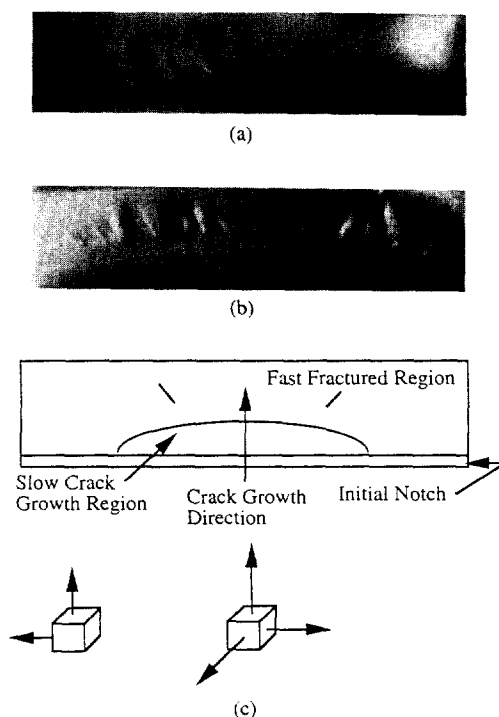

(a)

(b)

(c)

Figure 9. Fracture surfaces of inner notched (notch 2) as-received specimens at various load duration times. (a) t = t_1, (b) $t_2 > t_1$, and (c) approximate crack tip stress states.

The appearance of the slow crack growth fracture surfaces is typical of the fibrillated morphology, indicative of the slow crack growth being occurred through void nucleation and growth mechanisms applied to semicrystalline polymers. Hence the slow crack growth behavior observed at different residual stress states can be better understood by considering the behavior of hydrostatic (σ_0) and deviatoric (S_0) stress components at the notch tip, given in Equations 3 and 4, and how they are influenced by the presence of residual

$$\sigma_0 = \frac{(\sigma_{11} + \sigma_{22} + \sigma_{33})}{3} \tag{3}$$

$$S_0 = \frac{1}{6}[(\sigma_{11} - \sigma_{11})^2 + (\sigma_{22} - \sigma_{33})^2$$
$$+ (\sigma_{33} - \sigma_{11})^2 + \sigma_{23}^2 + \sigma_{13}^2 + \sigma_{12}^2]^{\frac{1}{2}} \tag{4}$$

stresses.

In general, S_0 is reduced when a multiaxial tensile stress of similar magnitude is created at the crack tip. This in turn can increase σ_0 which is the component of the total stress that drive the void nucleation and growth necessary for the slow crack growth. Thus, whether the crack growth occurs more or less readily depends on the stress condition near crack tip and the ratio, σ_0/S_0, is a good indicator for the rate of slow crack growth. Fig. 7c, 8d and 9c illustrate the approximate stress state envisioned for notch tips under zero (annealed), compressive and tensile residual stresses, respectively, with having the superimposed applied stress. For specimen with no residual stress (7c), the crack tip stresses are all tensile at the center and causes a normal plane strain constraint to exist, thus favoring cavitation and void formation and causes crack front to advance more rapidly at the center than at the edge, where a plane stress condition prevails. The magnitude of stress components at the crack tips occurred totally from the applied load. This is typical of the normal slow crack growth. For the outer notched as-received specimen (8d), the presence of circumferential and longitudinal compressive residual stresses at the center region of the crack front acts against the superimposed tensile stresses. As a consequence, σ_0/S_0 became reduced and thus delaying the crack growth. Since the compressive residual stress is equal-biaxial, it is likely that the total stress parallel to the crack front may even become compressive, as shown. σ_0/S_0 is higher at the crack front near the ring edge because the compressive residual stresses near the edges are relaxed as a result of sectioning the rings from the pipe. Thus, higher crack growth rate is expected near the edges, as shown. Similarly, the superposition of tensile residual stresses to the crack tip tensile stresses at the center region increases σ_0/S_0 ratio at the crack front,

in comparison to no residual stress condition, and thus increasing the tendency toward the slow crack growth (Fig. 9c). However, in the edge region, the crack growth is delayed because of the fact that the removal of tensile residual stresses during ring sectioning caused σ_0/S_0 to become reduced.

Some quantitative estimate of the crack tip stress field that drives the slow crack growth can be obtained for the annealed and as-received samples by calculating the stress intensity factor (K_I) given in Equation 5. The relationship between K_I and the crack speed (V) is also given in Equation 6.

$$K_I = \sqrt{\frac{E\, P^2 \phi}{2(1-\nu^2)}} \tag{5}$$

$$K_I \propto V^n \tag{6}$$

Here, E and ν are the material constants, n is a constant that depends on operating crack growth mechanism, and ϕ is the change of compliance
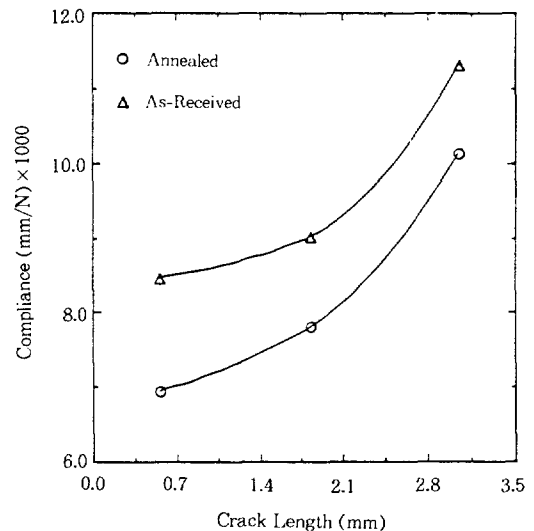

Figure 10. Compliance curves for outer notched as-received and annealed SCG ring specimens.

with crack length, which is obtained by the differentiation of the compliance curves shown in Fig. 10. Thus, for the initial crack length of 0.5 mm, and at given load P, the corresponding notch tip stress intensity factors were estimated as 300 and 550 $KPa \sqrt{m}$, for outer notched as-received and annealed specimens, respectively. The lower K_I value obtained for the as-received specimen clearly indicates the lower stress field available for driving the crack, as the crack tip was affected by the compressive residual stresses. This strongly demonstrates the applicability of the ring SCG specimen to slow crack growth investigations in the residually stressed plastic pipes, where the residual stress effects are directly determined.

CONCLUSIONS

A specimen and test method were developed to evaluate the slow crack growth behavior in polyethylene pipes under the influence of residual stresses. It required no treatment such as annealing to vary the residual stress state but utilized a naturally varying residual stress state, as they were produced during melt processing. It was determined that the compressive residual stresses reduced the rate of slow crack growth while tensile residual stresses increased the growth rate and eliminated the incubation period for the crack initiation. With tensile residual stress at the crack tip, the slow crack growth was accelerated up to about three times, compared to the compressive residual stress field. The physical evidence for this was observed from the fracture surfaces, which demonstrated the retarding and enhancing effects of compressive and tensile residual stresses, respectively, on the slow crack growth.

REFERENCES

1. A. Bhatnager, S. Choi, and L. J. Broutman, *Proc. of 10th Plastic Fuel Gas Pipe Symp.,* AGA, 324 (1987).
2. A. Bhatnager, S. Choi, and L. J. Broutman, GRI Report No. 86/0068 (1986).
3. B. Bell, S. Choi, and L. J. Broutman, *Proc. 8th Plastic Fuel Gas Pipe Symp.,* AGA, 57 (1983).
4. C. A. Sciammarella, Y. Yang, S. Choi, and L. J. Broutman, Illinois State OSWR Report No. 012-009 (1995).
5. L. J. Broutman, D. E. Duvall, and P. K. So, *Proc. 48th SPE-ANTEC,* 1495 (1990).
6. F. S. Uralil and L. E. Hulbert, GRI Report No. 85/0045, GRI (1985).
7. M. K. V. Chan and J. G. Williams, *Polymer,* **24,** 234 (1983).
8. N. Brown, *Proc. 9th Plastic Fuel Gas Pipe Symp.,* AGA, 283 (1985).
9. Y. Huang and N. Brown, *J. Polym. Sci.,* **28,** 2007 (1990).
10. X. Lu, Z. Zhou, and N. Brown, *Polym. Eng. Sci.,* **34,** 109 (1994).
12. J. J. Strebel and A. Moet, *J. Mat. Sci.,* **26,** 5671 (1991).
13. R. Frassine, M. Rink, and A. Pavan, *Proc. 9th Plastics Pipes,* 257 (1995).
14. S. Choi and L. J. Broutrman, *Polymer (Korea),* **21,** 71 (1997).
15. S. Choi and L. J. Broutman, *Proc. 9th Defor. Yield Frac. Symp.,* 48/1 (1994).
16. S. Choi and L. J. Broutman, *Polymer(Korea),* **21,** 93 (1997).
17. J. R. Leech, *Proc. 9th Plastic Fuel Gas Pipe Symp.,* 3 (1985).
18. S. P. Timoshenko, "Theory of Elasticity", 3rd ed., p. 136, McGraw-Hill, New York, 1970.
19. M. M. Frocht, "Photoelasticity", Vol. II, p. 193, John-Wiley & Sons, New York, 1948.